

Article

Design, Energy, Environmental and Cost Analysis of an Integrated Collector Storage Solar Water Heater Based on Multi-Criteria Methodology

Nektarios Arnaoutakis ¹, Andreas P. Vouros ², Maria Milousi ³, Yannis G. Caouris ², Giorgos Panaras ⁴ , Antonios Tourlidakis ⁴, Kyriakos Vafiadis ⁴ , Giouli Mihalakakou ⁵, Christos S. Garoufalidis ⁶ , Zacharias Frontistis ³ , Spiros Papaefthimiou ¹  and Manolis Souliotis ^{3,*} 

- ¹ School of Production Engineering & Management, Technical University of Crete, 73100 Chania, Greece; nec@dpem.tuc.gr (N.A.); spiros@pem.tuc.gr (S.P.)
- ² Department of Mechanical Engineering & Aeronautics, University of Patras, 26504 Patras, Greece; vouros@upatras.gr (A.P.V.); caouris@upatras.gr (Y.G.C.)
- ³ Department of Chemical Engineering, University of Western Macedonia, 50150 Kozani, Greece; mmilousi@uowm.gr (M.M.); zfrontistis@uowm.gr (Z.F.)
- ⁴ Department of Mechanical Engineering, University of Western Macedonia, 50150 Kozani, Greece; gpanaras@uowm.gr (G.P.); atourlidakis@uowm.gr (A.T.); kvafiadis@uowm.gr (K.V.)
- ⁵ Department of Environmental Engineering, University of Patras, 30100 Agrinio, Greece; pmichala@upatras.gr
- ⁶ Department of Material Science, University of Patras, 26504 Patras, Greece; garoufal@upatras.gr
- * Correspondence: msouliotis@uowm.gr; Tel.: +30-24610-56623



Citation: Arnaoutakis, N.; Vouros, A.P.; Milousi, M.; Caouris, Y.G.; Panaras, G.; Tourlidakis, A.; Vafiadis, K.; Mihalakakou, G.; Garoufalidis, C.S.; Frontistis, Z.; et al. Design, Energy, Environmental and Cost Analysis of an Integrated Collector Storage Solar Water Heater Based on Multi-Criteria Methodology. *Energies* **2022**, *15*, 1673. <https://doi.org/10.3390/en15051673>

Academic Editor: Dorota Chwieduk

Received: 27 January 2022

Accepted: 22 February 2022

Published: 23 February 2022

Publisher's Note: MDPI stays neutral with regard to jurisdictional claims in published maps and institutional affiliations.



Copyright: © 2022 by the authors. Licensee MDPI, Basel, Switzerland. This article is an open access article distributed under the terms and conditions of the Creative Commons Attribution (CC BY) license (<https://creativecommons.org/licenses/by/4.0/>).

Abstract: The paper presents a design and operation analysis of an Integrated Collector Storage (ICS) solar water heater, which consists of an asymmetric Compound Parabolic Concentrating (CPC) reflector trough, while the water tank comprises two concentric cylinders. The annulus between these vessels is partially depressurized and contains a small amount of water in the bottom of the outer vessel which dominantly contributes to the heat transfer from the outer to the inner cylinder. A multi-criteria optimization algorithm is applied to re-evaluate the design specifications of the parabolic surface, thus modifying the design of the entire ICS system and predict the necessary number of units for achieving the highest possible effectiveness with minimized fabrication costs and environmental impacts. The environmental footprint of the device is assessed through Life Cycle Assessment (LCA). The produced thermal energy in conjunction with the environmental and economic results are evaluated as a function of different configuration parameters regarding the water storage conditions, the solar radiation and the total pressure inside the annulus. The ultimate aim of the evaluation process is to offer new perspectives on the design principles of environmentally friendly and cost-effective devices with improved thermal performance.

Keywords: ICS solar water heater; multi-criteria decision analysis; Life Cycle Assessment (LCA); thermal energy analysis; environmental and economy profile

1. Introduction

Solar Water Heating (SWH) systems contribute to the reduction of greenhouse emissions during lifetime operation. Nowadays, different types of SWH systems are used, such as flat plate and evacuated tube thermosiphonic units (Flat Plate Thermosiphonic Units: FPTU; Evacuated Tube Thermosiphonic Units: ETTU) and forced circulating systems (Flat Plate Forced Circulating Units: FPFU; Evacuated Tube Forced Circulating Units: ETFCU) and Compound Parabolic Concentrating (CPC) reflectors in connection with storage tanks for domestic applications. Usually, CPC reflectors are adopted in Integrated Collector Storage (ICS) water heating systems [1,2].

Solar water heaters are considered “clean” and low-cost thermal energy systems. However, the cost of specific types of solar water heaters with high construction complexity has

increased rapidly, i.e., the combination of evacuated tube collectors with CPC-type reflectors could be such a reason for increased cost systems [3]. Souliotis et al. [4] and Singh et al. [5] analysed recent developments in the ICS solar systems and Papaefthimiou et al. [6] presented the developments in energy modelling and management of solar water heating systems during the last decade.

Several scientific studies have presented results on the environmental viability of such systems. Crawford et al. [7] focused on energy consumption and CO₂ emissions during the operation of FPTU water heaters, while Kalogirou [8] presented the environmental and economic analysis of a thermosiphon SWH used for domestic applications in Cyprus with two types of backups (electricity and diesel). Focusing on SWH systems, Yin Hang et al. [9] compared their economic and environmental performance with those conventional for typical residential buildings in the United States, while Colle et al. [10] studied both SWH and PV systems.

Several studies have employed Life Cycle Assessment (LCA) methodology to evaluate the environmental profile of solar thermal systems throughout their whole life cycle. The energy and environmental balance throughout the entire life cycle of flat plate solar collectors were initially presented by Ardenne et al. [11], while Crawford and Treloar [12] estimated the embodied energy, the greenhouse gas (GHG) emissions, and the payback period during the whole life cycle of installed solar systems in two Australian cities. The environmental impact assessment of the entire life cycle of an innovative prototype vacuum tube solar collector using Phase Change Material (PCM) was presented by Jachura and Sekret [13]. Furthermore, Karasu and Dincer [14] used a cradle-to-grave LCA to analyse integrated borehole type thermal energy storage (TES) systems in Canadian buildings. Lamnatou et al. in [15–17] presented a comprehensive LCA studies analysing the environmental profile of solar devices, either stand alone or Building Integrated Solar Thermal (BIST) systems. The results revealed a high dependence on the materials used for the concentrator/storage tank, and the need for improved recycling processes.

The optimal design of SWH systems aims at low-cost systems with improved thermal behaviour and environmental footprint. An optimization process can focus on the design or/and operation of solar thermal systems in various applications. In this direction, Hobson and Norton [18] proposed a design algorithm for direct thermosiphon SWHs by presenting a characteristic curve for domestic SWHs in order to predict the annual solar fraction for a validated numerical simulation model. On the other hand, Gordon and Rabl [19] proposed an optimization in the design of industrial solar plants without heat storage, with a focus on the lowest fabrication cost. Frei and Vogelsanger [20] presented an optimum design methodology for solar thermal systems for domestic hot water and space heating, including comparative results to more traditional designs. In the work of Lund and Peltola [21], the predesign and the optimization of solar heating systems with seasonable storage were studied, demonstrating a simulation design tool which evaluates the energy system's size and dimensions. In addition, Abdel-Malek [22] described the optimum design of SWHs through the analysis of the design parameters depending on the solar incidence for various areas and the demand for hot water. De Winter [23] presented optimum designs for SWH with different tank designs for a single-family home.

The majority of existing literature regarding the optimization of solar thermal systems does not take into account the anticipated environmental footprint of the proposed systems. However, Ko [24] presented an optimization method for the design of a SWH system on the basis of the Life Cycle Cost (LCC) methodology. A genetic algorithm was employed to optimize the configuration and sizing of three constraint conditions, including energy balance, solar fraction and available space to install solar collectors. Furthermore, Patrčević et al. [25] presented a methodology for conducting a cost-optimal energy performance calculation of a SWH system, used for space heating and domestic hot water needs. The calculation was based on dynamic hourly methods dealing with storage-tank water temperature calculations and provided proposals for modifications in order to overcome the observed ambiguities and shortcomings.

The present work presents a detailed study of an ICS system comprising two concentric cylindrical tanks placed horizontally and an asymmetric CPC reflector. The primary objective of the paper is to identify the optimal sizing of the ICS system and to evaluate the optimum dimensions of each part of the reflector. The proposed optimization technique aims at fulfilling four basic criteria: (i). the highest mean daily efficiency, (ii). the lowest water tank's thermal losses at night, (iii). the minimization of the fabrication cost, and (iv). the reduction of environmental impacts throughout the entire life cycle of the device, for different geographic locations of Greece. The second objective of this work is to provide a detailed and comparative energy, cost, and environmental analysis in various operational modes for the proposed ICS units. The economic profile of the models is studied using the Net Present Value (NPV) and the simple payback period, in order to estimate the economic viability of such systems, especially when installed on islands.

The adopted optimization process is not only novel but also offers new perspectives in the design principles of environmentally friendly and cost-effective devices. Parameters such as the size of the reflector (and its geometry) and the required number of units for optimum operation, are all taken into consideration in the pursuit of achieving the combined targets of minimum environmental footprint and maximum performance. To the best of our knowledge, the existing literature on domestic SWH systems mainly focuses on either specific design aspects of devices (noting that the optical analysis is not gaining the interest of most researchers) or on the LCA analysis. The combination of both these evaluation aspects in a single optimization procedure has not been previously reported.

The layout of the paper is as follows. Section 2 presents all technical details about the design, the operational concept, the environmental and economic profile of the of the proposed ICS system. Additionally, the multi-criteria design problem is presented alongside the proposed optimization technique. Section 3 contains the optimum dimensions for the parabolic parts and the comparison of the results, while in the last section, the conclusions of the study are discussed.

2. Design, Energy, and Environmental Analysis

2.1. Design and Operation Concept of the ICS System

Souliotis et al. [26,27] proposed the reference ICS model, illustrated in Figure 1. The water storage consists of two cylindrical vessels, one inside the other. In particular, the annulus between the two cylinders is partially depressurized containing a small amount of water in the bottom (4ℓ at 15 °C) which acts as PCM. PCM materials can improve the thermal behaviour of solar devices by reducing thermal losses [28–34]. The vapor that is produced creates a heat diode transfer mechanism from the outer vessel to the inner water storage tank (Figure 1).

The design details and the operation of the specific device have been described in the literature [26]. The quantification, by means of suitable measurements, of the temperature stratification of the tank is important for the evaluation of the system's performance. This can be ascertained using a grid of thermocouples positioned inside the inner tank as indicated in Figure 2 [27] (positions: plane 1 (1,1), (1,2), (1,3), plane 2: (2,1), (2,2), (2,3) and plane 3: (3,1), (3,2), (3,3)). Inside the annulus, three thermocouples were located in positions (i), (ii), and (iii). The pressure sensor (Figure 2) was placed close to the evacuation port and the nearest thermocouple pipe port [27]. For the studied procedure eight values of the total pressure within the annulus (at the lowest possible temperature values of water—vapor in the annulus) have been examined: 86 ± 2 mbar (at 19.5 ± 1 °C), 140 ± 3 mbar (at 26.0 ± 1 °C), 245 ± 6 mbar (at 24.0 ± 1 °C), 340 ± 8 mbar (at 25.0 ± 1 °C), 490 ± 11 mbar (at 23.0 ± 1 °C), 670 ± 16 mbar (at 22.0 ± 1 °C), 790 ± 18 mbar (at 20.0 ± 1 °C) and 990 ± 23 mbar (at 24 ± 1 °C) [27].

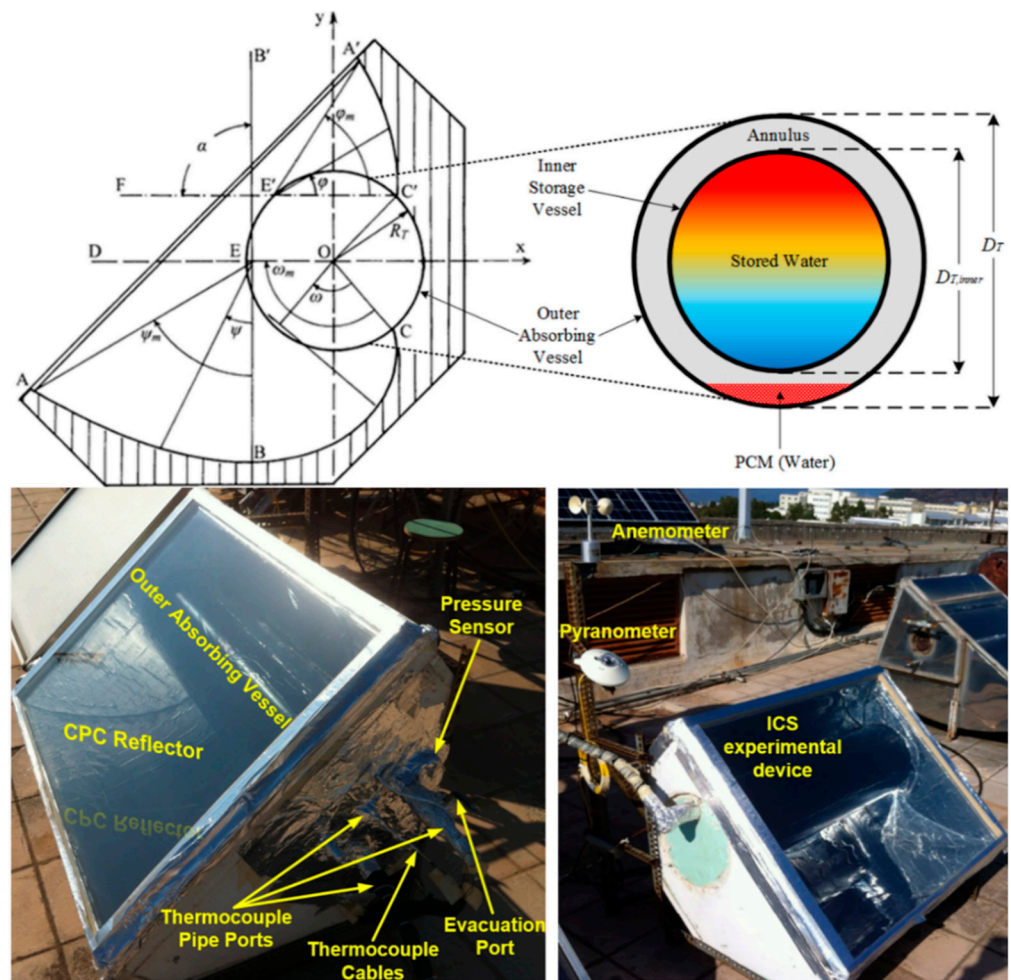


Figure 1. ICS water heater with asymmetric reflector and double wall tank [26,27].

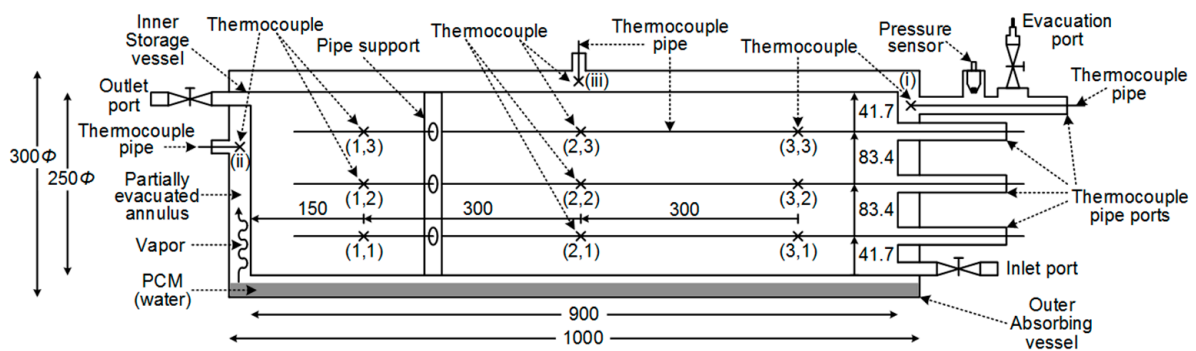


Figure 2. Cross-section of the inner storage vessel, outer absorbing vessel, numbering/positioning of the thermocouples within the inner storage vessel and the annulus positioning of the pressure sensor, inlet, outlet, evacuation, and thermocouple pipe ports [27].

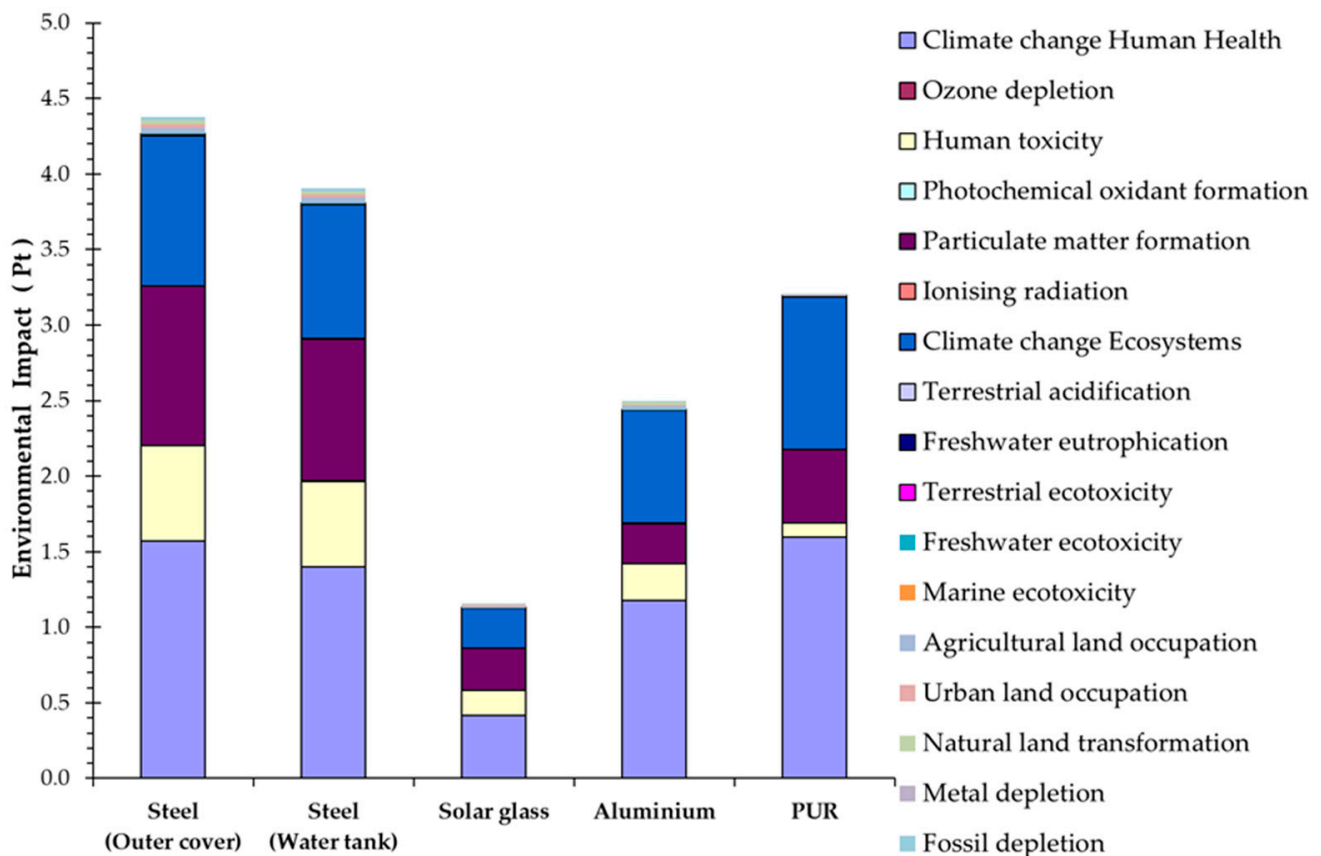
2.2. Environmental and Energy Analysis during Fabrication and Installation Phases

The ICS device (Figure 1) is mainly composed of five parts: the casing, the insulation, the asymmetric parabolic reflector, the solar glass cover, and two concentric water tanks. The design and construction details of a similar system are presented in previous work by Arnaoutakis et al. [35]. Table 1 presents all quantities (in kg) of the employed materials for the system in Figure 1.

Table 1. Quantified technical details of employed materials for the ICS system.

Absorbing Reflector		Water Tank		Other Parts	
Material	Mass (kg)	Material	Mass (kg)	Material	Mass (kg)
Steel	44.47	Steel	29.40	Plastic tube	2
Aluminium	6.49	Magnesium	0.10	Glass fibre	2
Solar Glass	8.74				
PUR	12.02				
Total	71.72		29.50		4

The environmental and energy analysis of the studied system is investigated through the LCA method, which follows the ISO standards 14040, 14044 [36,37] and is implemented with SimaPro 8.5 [38] and ecoinvent 3.4 database [39]. The environmental impact assessment methodology used is Recipe Endpoint 2016 Hierarchist [40]. Figure 3 summarizes the environmental footprint of the studied system.

**Figure 3.** Aggregated environmental impacts during the ICS fabrication and installation phase.

As presented in Figure 3, the highest environmental impacts are caused by the extensive use of steel for the construction of the outer cover and the water tank and are mainly assigned to the following impact categories (with decreasing magnitude): climate change, human health, climate change ecosystems, particulate matter formation and human toxicity [39]. The first two categories increase the greenhouse gas emissions that affect climate change, while the last two contribute to potential lung and respiratory problems in human health [39]. Similarly, the necessity for using large quantities of polyurethane (PUR) during the fabrication process mainly influences the climate change category, while the generated wastes from the formulation of the thermal insulation inside the casing affect the particulate matter formation and human toxicity categories [39]. The rest of the materials are assigned with a relatively low impact score. The total energy demands during the

fabrication and installation of the ICS system is 43.83 MJ (~12.2 kWh), focusing on the collector with 10.08 MJ (~2.8 kWh), the water tank with 27.73 MJ (~7.7 kWh), the support system with 5.5 MJ (~1.5 kWh) and the installation with 0.52 MJ (~0.15 kWh) [35]. All the above form the production cost during the fabrication and installation phases, with a total value of approximately EUR 292, the production electricity cost EUR 2, the material cost EUR 190 and the salary cost EUR 100 [35].

2.3. Energy, Environmental and Economic Analysis in Operation Mode

The energy analysis, throughout the operation phase, can provide the produced thermal quantity of the SWH during a yearly operation period [41]. The annual produced thermal energy ($Q_{THEYear}$) of the studied system (Figure 1) was evaluated by the following equation [42]:

$$Q_{THEYear} = Gains - Losses = \sum_{k=1}^{k=12} \{D_k \cdot A \cdot t \cdot [G_m \cdot \eta_d(\psi_m, \varphi_m, B, C) - U_S(D, F) \cdot (T_{i,m} - T_{\alpha,m})]\}, \quad (1)$$

where:

$Q_{THEYear}$: produced thermal energy, in MWh/Year

A : absorbing surface, in m^2

G_m : mean daily solar radiation on the aperture plane, in W/m^2

$\eta_d(\psi_m, \varphi_m, B, C)$: mean daily efficiency for the time period t of the day

$U_S(D, F)$: thermal loss coefficient during night operation, in $W \cdot m^{-2} \cdot K^{-1}$

$T_{i,m}$: mean initial water temperature during night operation, in $^{\circ}C$

$T_{\alpha,m}$: mean ambient temperature during night operation, in $^{\circ}C$

D_k : number of days of each month

k : an index for each month for one-year operation period of the system

The angles ψ_m and φ_m are the maximum reflector's angles, as indicated in Figure 1, while B , C , D , and F are not constant parameters. The parameters $\eta_d(\psi_m, \varphi_m, B, C)$ and $U_S(D, F)$ in Equation (1) have been addressed analytically by Souliotis et al. [26,27], Souliotis and Tripanagnostopoulos [41], Rabl [43] and Arnaoutakis et al. [44].

Apart from the energy analysis, the environmental and economic studies can provide information about the impact and the viability of a solar thermal energy system during the entire operation period. To approach and investigate both, RETScreen Expert, a dedicated energy management software [45] is utilised. RETScreen Expert is a software that helps decision-makers to determine the technical and financial feasibility of potential renewable energy, energy efficiency, and cogeneration (combined heat and power) projects. Each project goes through a five-step analysis that includes energy, cost, emission, financial, and sensitivity/risk sub-elements.

The net annual greenhouse emission reduction for the ICS system of Figure 1 is approximated by using the test results from various cases of different FPTU systems in the RETScreen computational tool. All these tests were performed based on the weather data of Greece.

The main economic parameters are the Net Present Value (NPV) and the payback period. In finance, the NPV or the Net Present Worth (NPW) [46] is an indicator of the profitability of a project or product that is calculated by subtracting the Present Values (PV) of cash outflows (including initial cost) from the present values of cash inflows over a period of time [47]. Incoming and outgoing cash flows can also be described as benefit and cost cash flows, respectively [47]. The following equation is the formula for the NPV calculation:

$$NPV = \sum_{t=1}^T \frac{C_t}{(1+r)^t} - C_0 \quad (2)$$

where:

C_t : net cash inflow during the period t

C_o : total initial investment costs
 r : discount rate
 t : number of time periods.

The payback period is the time required to recover the cost of a given investment and is an important determinant of whether to undertake the project [48]. Typically, the payback period is calculated via the expression:

$$\text{Payback Period} = \frac{\text{Cost of Project}}{\text{Annual Cash Inflows}} \quad (3)$$

2.4. Design Analysis

The main objective of this subsection is the fabrication of totally new water heaters with higher efficiency without significantly increasing the production cost of the system. The design details of the studied system have already been described in the literature [26,49]. The reflector is composed of two asymmetric parabolic parts ((AB), ($C'A'$)) and there is only one involute part, the (BC), respectively. Taking into account the geometry of Figure 1, the optimization problem is described by the following set of equations:

$$\left\{ \begin{array}{l} \max[z \cdot n_d(\psi_m, \varphi_m, B, C)] \\ \max[-(z \cdot U_S(D, F))] \\ \max[-(z \cdot C_P(\psi_m, \varphi_m))] \\ 58.24^\circ \leq \psi_m < 90^\circ \\ 57.95^\circ \leq \varphi_m < 90^\circ \\ 0 \leq B \leq 7.03 \\ 0 \leq C \leq 4.95 \\ 0 \leq D \leq 6.08 \\ 0 \leq F \leq 0.024 \\ 1 \leq z \leq e \\ 0.74 \leq \frac{z \cdot \left(\frac{Q_{THE}}{Year}(\psi_m, \varphi_m, B, C, D, F) \right)}{3.6 \cdot 10^9} \leq f \end{array} \right. \quad (4)$$

A detailed description of a similar design problem was presented by Arnaoutakis et al. [44]. Here, the main difference is the existence of three objective functions instead of two: mean daily efficiency $n_d(\psi_m, \varphi_m, B, C)$, thermal loss coefficient $U_S(D, F)$ and production cost. In addition, this similar design problem has been considered for the case of only one ICS unit, with the values of the involved parameters (B, C) being kept fixed [44]. In the present work, the parameters B, C, D , and F involved in Equations (1) and (4) are not constant but vary between lower and upper limits, which were defined by previous experimental studies in ICS systems [26,49]. These parameters, along with the angular parameters ψ_m and φ_m (maximum reflector's angles as indicated in Figure 1) and the parameter z (number of the proposing installed ICS units in the building), represent the decision variables for the optimization problem of Equation (4). The objective is to find the size of the system of Figure 1, along with the number of proposed ICS units, which produces the maximum possible amount of thermal energy, whilst at the same time keeping the production cost to a minimum value. The first two objective functions are similar with the coefficients $n_d(\psi_m, \varphi_m, B, C)$ and $U_S(D, F)$, which have been described in Section 2.3. In addition, the quantity ($-C_P(\psi_m, \varphi_m)$) of the third objective function have already been analysed in the existing literature [43].

Based on the geometry of Figure 1 and the analysis of the studies of Souliotis et al. [26], Arnaoutakis et al. [44] and Tripanagnostopoulos and Souliotis [49], the optimum horizontal

and vertical dimensions for the parabolic parts (AB) and ($C'A'$), respectively, are expressed using the following formulas:

$$\begin{aligned} d_{AB, X} &= \frac{-R_T \left[1 + \left(\frac{3\pi}{2} \right) \cdot \sin \psi_m \right]}{1 + \cos \psi_m} \\ d_{AB, Y} &= \frac{-R_T \cdot \left(\frac{3\pi}{2} \right) \cdot \cos \psi_m}{1 + \cos \psi_m} \end{aligned} \quad (5)$$

$$\begin{aligned} d_{C'A', X} &= R_T \left[\frac{\sqrt{2}}{2} - \frac{(2\sqrt{2}) \cdot \cos \varphi_m}{1 + \cos \varphi_m} \right] \\ d_{C'A', Y} &= R_T \left[\frac{\sqrt{2}}{2} + \frac{(2\sqrt{2}) \cdot \sin \varphi_m}{1 + \cos \varphi_m} \right] \end{aligned} \quad (6)$$

Similarly, [26,44,49–51] the dimensions (lengths) for the parabolic (AB), ($C'A'$) and the involute part (BC), respectively, are calculated as:

$$(AB) = \frac{1}{2} \cdot \left[\begin{aligned} &\frac{1}{2} \cdot \sqrt{\left(2 \cdot \frac{R_T [1 + (4.71 \cdot \sin \psi_m)]}{1 + \cos \psi_m} \right)^2 + 16 \cdot \left(\frac{R_T \cdot 4.71 \cdot \cos \psi_m}{1 + \cos \psi_m} \right)^2} - \\ &\frac{\left(2 \cdot \frac{R_T [1 + (4.71 \cdot \sin \psi_m)]}{1 + \cos \psi_m} \right)^2}{\frac{R_T \cdot 4.71 \cdot \cos \psi_m}{1 + \cos \psi_m}} \cdot \ln \left(\frac{-R_T \cdot 18.84 \cdot \cos \psi_m + \sqrt{\left(2 \cdot \frac{R_T [1 + (4.71 \cdot \sin \psi_m)]}{1 + \cos \psi_m} \right)^2 + 16 \cdot \left(\frac{R_T \cdot 4.71 \cdot \cos \psi_m}{1 + \cos \psi_m} \right)^2}}{2 \cdot \frac{-R_T [1 + (4.71 \cdot \sin \psi_m)]}{1 + \cos \psi_m}} \right) \end{aligned} \right] \quad (7)$$

$$(BC) = \frac{R_T}{2} \cdot \omega_m^2 \quad (8)$$

$$C'A' = \frac{1}{2} \cdot \left[\begin{aligned} &\frac{1}{2} \cdot \sqrt{\left(2 \cdot R_T \left[\frac{\sqrt{2}}{2} + \frac{(2\sqrt{2}) \cdot \sin \varphi_m}{1 + \cos \varphi_m} \right] \right)^2 + 16 \cdot \left(R_T \left[\frac{\sqrt{2}}{2} - \frac{(2\sqrt{2}) \cdot \cos \varphi_m}{1 + \cos \varphi_m} \right] \right)^2} + \\ &\frac{\left(2 \cdot R_T \left[\frac{\sqrt{2}}{2} + \frac{(2\sqrt{2}) \cdot \sin \varphi_m}{1 + \cos \varphi_m} \right] \right)^2}{8 \cdot R_T \left[\frac{\sqrt{2}}{2} - \frac{(2\sqrt{2}) \cdot \cos \varphi_m}{1 + \cos \varphi_m} \right]} \cdot \ln \left(\frac{4 \cdot R_T \left[\frac{\sqrt{2}}{2} - \frac{(2\sqrt{2}) \cdot \cos \varphi_m}{1 + \cos \varphi_m} \right] + \sqrt{\left(2 \cdot R_T \left[\frac{\sqrt{2}}{2} + \frac{(2\sqrt{2}) \cdot \sin \varphi_m}{1 + \cos \varphi_m} \right] \right)^2 + 16 \cdot \left(R_T \left[\frac{\sqrt{2}}{2} - \frac{(2\sqrt{2}) \cdot \cos \varphi_m}{1 + \cos \varphi_m} \right] \right)^2}}{2 \cdot R_T \left[\frac{\sqrt{2}}{2} + \frac{(2\sqrt{2}) \cdot \sin \varphi_m}{1 + \cos \varphi_m} \right]} \right) \end{aligned} \right] \quad (9)$$

where ψ_m , φ_m are the angular parameters, constituting also two of the decision variables of the optimization problem, R_T is the radius of the water storage and ω_m is the maximum angle for the involute part (BC) of the reflector. The angle ω_m does not belong to the decision variables of the problem and it takes the specific value $\omega_m = 135^\circ$, as provided by the existing literature [26,49]. The Equation (4) are solved using a multi-criteria design analysis method that optimizes a group of nonlinear objective functions and is based on an existing algorithm used in problems with several decision variables [52,53].

The entire optimization procedure is performed with an inhouse FORTRAN and Visual Basic code. The program code is interfaced with a database containing parameters for various materials (e.g., optical and thermal attributes and prices per preference unit) [26,44,54–57]. In addition, the database includes weather data of different Greek locations [58] and estimations of the hot water consumption's dependency on the number of occupants in the installation building. The code supports different reflector types (symmetric or asymmetric) and water tank capacities. Other sub-functions of the algorithm are the evaluation of the produced thermal energy using Equation (1), the greenhouse gas emissions in operation mode for the designed ICS system, and the techno-economical procedure, using Equations (2) and (3) for the calculation of the NPV and Payback period parameters. The annual emission reduction of the redesigned ICS devices and the consumption's dependency with the number of occupants in the building are approached using the RETScreen software and various test results of the systems, which are considered to be installed in Greek territory. The materials, which are derived from the database, are classified through the following environmental criteria:

- + + +: Environmentally friendly materials.
- - + +: Materials with more pollutants but not very harmful to the environment.
- - - +: Less environmentally friendly materials.
- - - -: Materials with damaging environmental behavior.

The above categorization considers impacts during fabrication and installation phases and is depicted taking into account the environmental footprint of Figure 3 and the Recipe Endpoint 2016 Hierarchist Methodology.

Additional operations of the program refer to the prediction of the optimum number of the solar thermal water units that will be installed in the building and the evaluation of the produced thermal energy and the greenhouse gas emissions during operation phase for all the designed devices. The lower and upper limits, especially for the parameter e in the 7th constraint of the Equation (4), referring to the prediction of the installed units, are based on the following assumption: the water consumption depends on the domestic hot water needs per occupant (50–60 ℓ /day). If that energy reaches some very low values, the designed “one” unit cannot cover the hot water needs of that selected by the input menu occupants, and it is necessary to fabricate more than one device which will be installed in the studied residence (declared in the optimization problem as the coefficient e in the upper limit of the 7th constraint). The same limits in the last constraint (which are expressed in MWh/Year) are based on similar assumptions (using RETScreen’s program existing case studies for solar thermal systems) such as the parameter f depending on hot water consumption per occupant. In addition, the quantity: $Q_{THEYear}(\psi_m, \varphi_m, B, C, D, F)$ of the same constraint is influenced by the desired water temperature, which is also related to the number of people that will use the ICS system.

Thus, in the optimization procedure, if the suggested unit is highly efficient, the specific device can produce the appropriate amount of thermal energy for all the occupants in the building and the algorithm does not allow the making of other water heaters, except the one which has already been designated by the code.

Using a Graphical User Interface (GUI environment), the program extracts the optimum reflector’s geometry, the environmental impacts along the entire life cycle of the device, the tank’s geometry, the mean daily efficiency, the thermal loss coefficient, the production cost of the system, and the appropriate number of the ICS units. The output form of the algorithm supports optical design plans that describe the optimum geometry for the entire solar water heater. These plans can help the fabrication of specific devices in the industry. The flow charts that summarize the above procedures are depicted below (Figures 4 and 5).

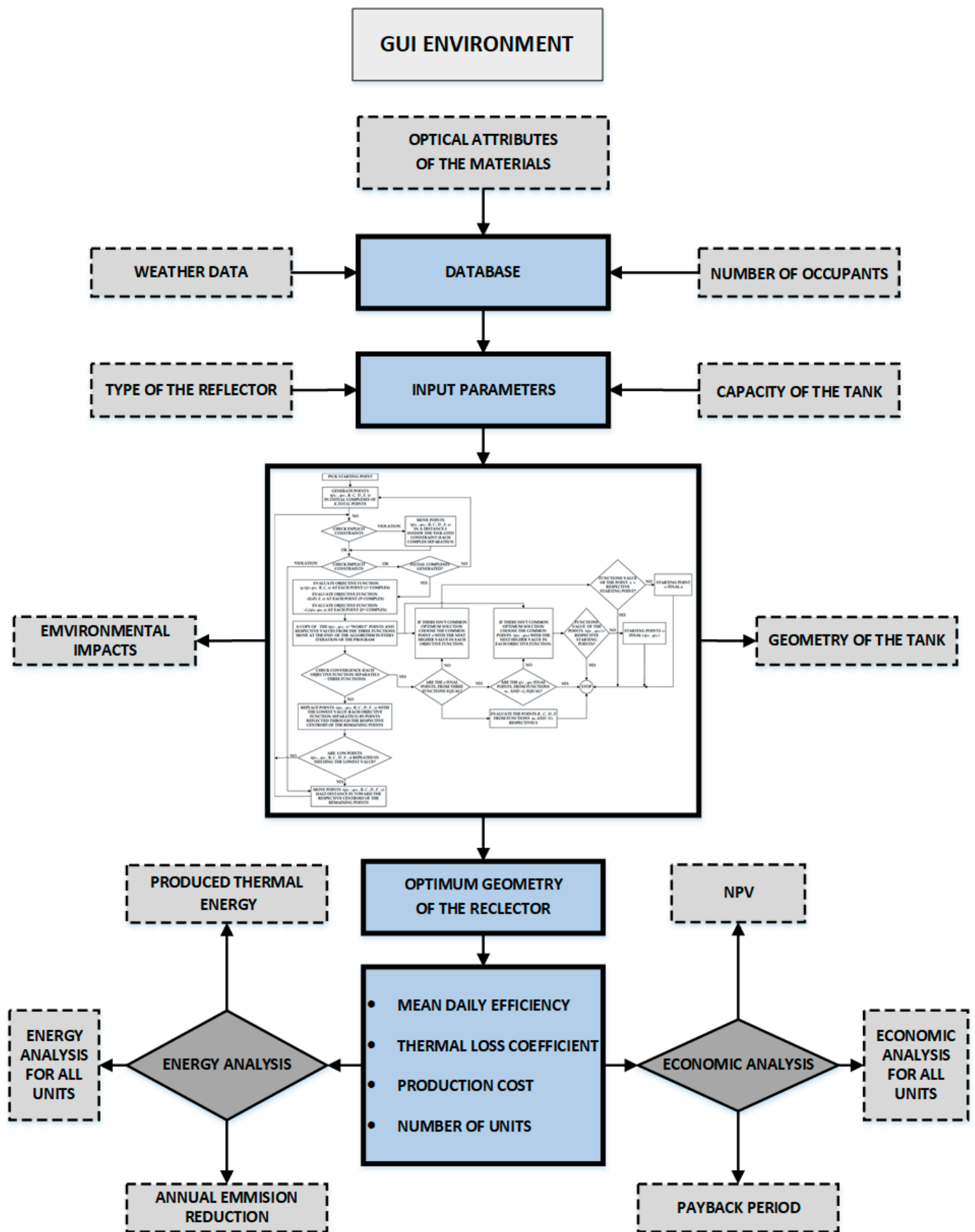


Figure 4. Flow chart of the program.

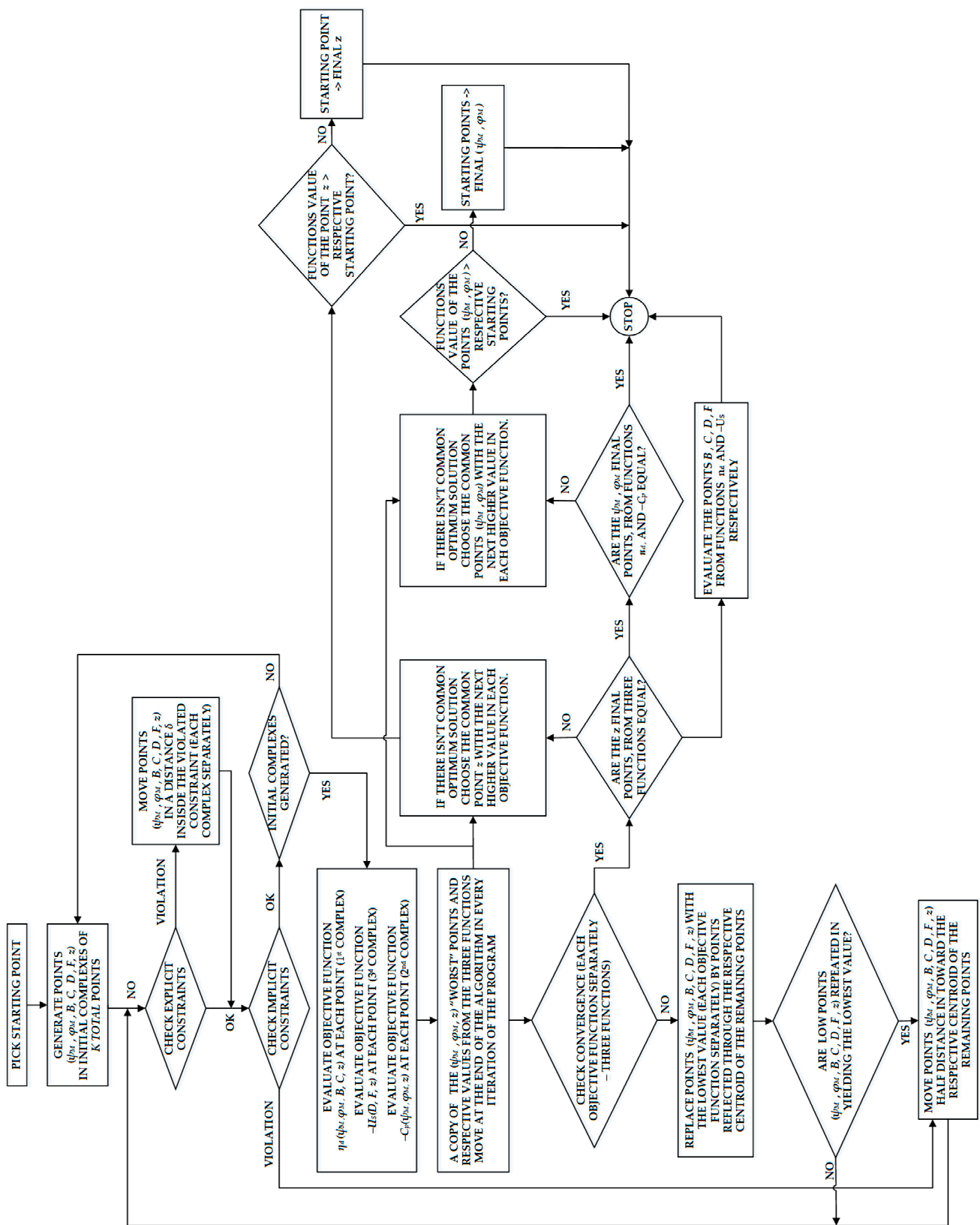


Figure 5. Analytical presentation of the multi-criteria design analysis methodology (flow chart that is included in the central image of Figure 4).

The employed multi-criteria design analysis method (Figure 5) maximizes the objective functions: $[z \cdot n_d(\psi_m, \phi_m, B, C)]$, $[-(z \cdot U_s(D, F))]$ and $[-(z \cdot C_p(\psi_m, \phi_m))]$. The

limits of the method are defined by the following constraints: $58.24^\circ \leq \psi_m < 90^\circ$, $57.95^\circ \leq \varphi_m < 90^\circ$, $B \leq 7.03$, $0 \leq C \leq 4.95$, $0 \leq D \leq 6.08$, $0 \leq F \leq 0.024$, $1 \leq z \leq e$ and $0.74 \leq \left[\frac{z \cdot \left(Q_{\text{Year}}^{\text{THE}}(\psi_m, \varphi_m, B, C, D, F) \right)}{3.6 \cdot 10^9} \right] \leq f$. The defined limits of the above constraints depend on the decision variables of the problem.

A similar design approach has already been referred to in the existing literature [42,50], with significant differences in various points that are described analytically in the following paragraphs.

In the above problem, three original “complexes” of $K \geq N + 1$ points each are created. N is the number of decision variables of the problem (in the existing case $N = 7$), consisting of a feasible starting point. The variables ψ_m, φ_m are common in two of the three “complexes” (these two complexes correspond to the functions $n_d(\psi_m, \varphi_m, B, C, z)$ and $-C_p(\psi_m, \varphi_m, z)$) and the variable z is common in all three “complexes”. $K - 1$ additional point for each “complex”, generated from random numbers. Constraints for all the independent variables are given by the following formulas:

$$\psi_{m,i,j} = g_1 + r_{ij} \cdot (h_1 - g_1) \quad (10)$$

$$\varphi_{m,i,j} = g_2 + r_{ij} \cdot (h_2 - g_2) \quad (11)$$

$$B_{i,j} = g_3 + r_{ij} \cdot (h_3 - g_3) \quad (12)$$

$$C_{i,j} = g_4 + r_{ij} \cdot (h_4 - g_4) \quad (13)$$

$$D_{i,j} = g_5 + r_{ij} \cdot (h_5 - g_5) \quad (14)$$

$$F_{i,j} = g_6 + r_{ij} \cdot (h_6 - g_6) \quad (15)$$

$$z_{i,j} = g_7 + \text{Int} \left(r_{ij} \cdot \frac{h_7 - g_7}{10} \right) \quad (16)$$

where $i = 1, 2, \dots, N$ and $j = 1, 2, \dots, K - 1$ and r_{ij} are random numbers varying between 0–0.4 for Equations (10) and (11), 0.9–1.0 for Equations (12)–(15), and 3–10 for the last formula. In addition, h_1 to h_7 and g_1 to g_7 are the upper and lower limits of the nonlinear inequality constraints of the optimization problem, as presented in Equation (4).

Based on the study of Arnaoutakis et al. [44], the feasible starting point was related to the constraints $58.24^\circ \leq \psi_m < 90^\circ$ and $57.95^\circ \leq \varphi_m < 90^\circ$. In the specific case, there is an additional point (which similarly was related to constraint $1 \leq z \leq e$). Thus, in order to locate this point, random numbers (between 0–0.4: first two equations, 0.9–1.0: Equations (12)–(15), and 1–10: the last formula) are used for the parameter r_{ij} . The optimum solution may be lower or equal to the starting point, but the final decision will be provided by the optimization methodology of Figure 5. In addition, it is necessary that the random numbers r_{ij} in Equation (16) be in integer form, such as the result of the formula: $r_{ij} \cdot \frac{h_7 - g_7}{10}$ (*Int*: the first three letters of the word “Integer”). If the result is decimal, the integer part of the above calculation is selected.

The algorithm evaluates, except for the variables ψ_m, φ_m (optimum reflector’s angles and optimum number of the installed ICS units), the parameters B, C, D , and F , which define the mean daily efficiency and the thermal loss coefficient of the studied ICS system.

The selected configuration of the reflector and the water tank is defined by the input menu using the GUI environment (Figure 4), which also contains information about the materials of the system’s components, the climate conditions of the geographical area, and the number of people that will use the specific solar thermal system. Next, two choices are available from the program:

- The energy analysis option, which calculates the produced thermal energy during the entire life cycle of the system and is accompanied by the evaluation of the annual emission reduction during its operation.

- The economic analysis choice, which can provide information about the profit of the investment.

The total produced thermal energy from all the designed ICS units for a house with four occupants is exhibited (using the program) by the following equation:

$$Q_{TOTAL} = z \cdot Q_{THE/Year} \quad (17)$$

where z is the number of the ICS units in the building and $Q_{THE/Year}$ is the produced thermal energy (MWh/Year) for a single designed unit.

The input parameters for the designed ICS systems are the type of the reflector, the capacity of the water tank, the type of the constructive materials, the meteorological data of the installation area, the number of occupants in the building, and the desired temperature of the water storage. The algorithm approaches the annually produced thermal energy of the geographic location in "Athens" that is set as a reference value for the designed ICS units (the experimental study of the prototype ICS device [26] took place in the city of Patra's which belongs in the "Athens" climate zone [58]). Thus, the designed ICS unit will be able to meet the domestic hot water needs of a house with four occupants located in the "Athens" area. Using the above assumption [27], the code considers five cases for the initial total pressure of partial vacuum within the annulus of the water storage, applying them in the existing multi-criteria design analysis methodology:

- 86 ± 2 mbar (at 19.5 ± 1 °C)
- 245 ± 6 mbar (at 24.0 ± 1 °C)
- 490 ± 11 mbar (at 23.0 ± 1 °C)
- 670 ± 16 mbar (at 22.0 ± 1 °C)
- 990 ± 23 mbar (at 24 ± 1 °C)

3. Results

The main goal of the entire procedure is to find the ICS design with the lowest cost that presents almost the same mean daily efficiency and thermal loss coefficient with conventional FPTU devices, which are competitive systems to the ICS ones. The water storage volume was set at 48.18ℓ [27] for all the redesigned devices and the materials for the reflector and the tank were chosen to be aluminium and steel (materials which are used in Souliotis et al. studies [26,27]), respectively. After the completion of the simulation procedure, the optimum dimensions for the parabolic parts (AB) and ($C'A'$) of the reflector (which were evaluated through the maximum angles ψ_m and φ_m , respectively, as indicated in Figure 1 and Equations (7) and (9)), are depicted in Figure 6.

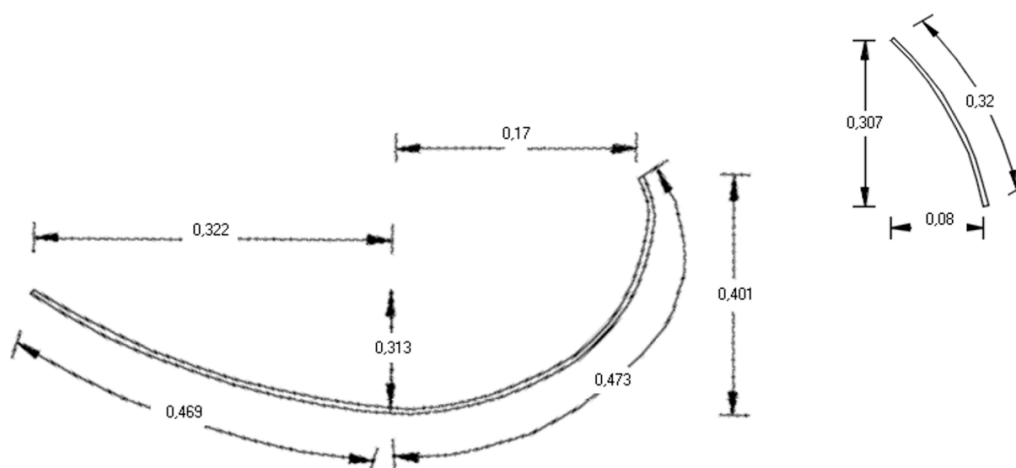


Figure 6. Optimum dimensions (in m) for the design reflector parabolic parts (AB) and ($C'A'$).

Next, using CAD (Computer Aided Design) software, two additional rectangular surfaces are evaluated. These geometrical shapes will be located (hypothetically) in the two parts of the reflector in order to formulate the scale for the parabolic part of the CPC surface in the CAD environment (Figures 7 and 8, respectively). It is considered that there is not any modification in the dimensions of the involute part [44], as discussed above for the ω_m angular parameter.

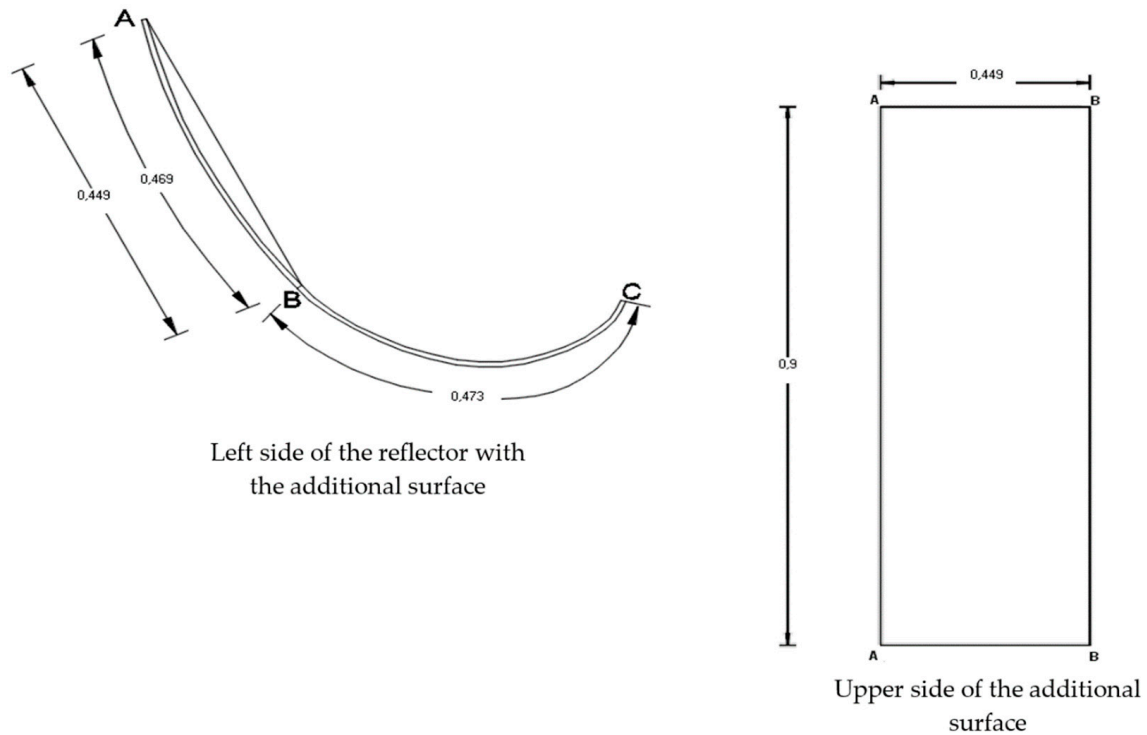


Figure 7. Dimensions (in m) for the additional surface, which will be hypothetically located in the left part of the reflector (CAD environment).

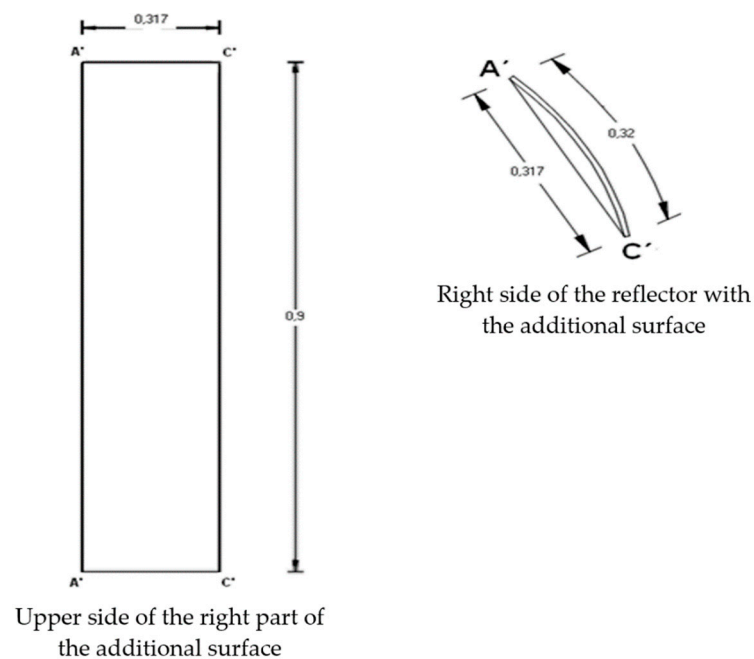


Figure 8. Dimensions (in m) for the additional surface, which will be hypothetically located in the right part of the reflector (CAD environment).

The above methodology (applied in industry) can produce different reflectors in a very short time with larger or smaller parabolic parts, compared with a prototype parabolic shape which was derived from the studies by Souliotis and Tripanagnostopoulos [26,27]. The derived designed drawings by this method can cooperate with a Computerized Numerical Control (CNC) machine in order to cut and bend the metal sheeting, which will be used in the fabrication of the studied reflector.

The aggregate results (of the programming code for a single ICS unit) for the mean daily efficiency and the thermal loss coefficient are depicted in Figures 9 and 10, respectively, compared with similar configurations (for the initial total pressure of partial vacuum within the annulus of the water storage) of the reference ICS model [27].

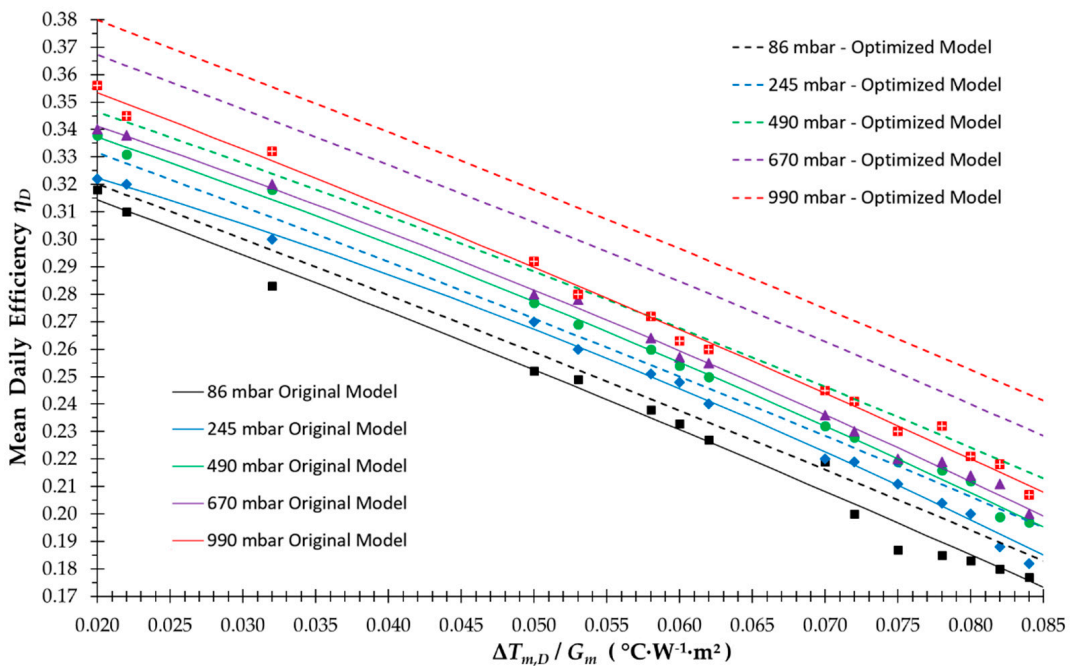


Figure 9. Variation of the mean daily efficiency for the optimized and reference ICS models.

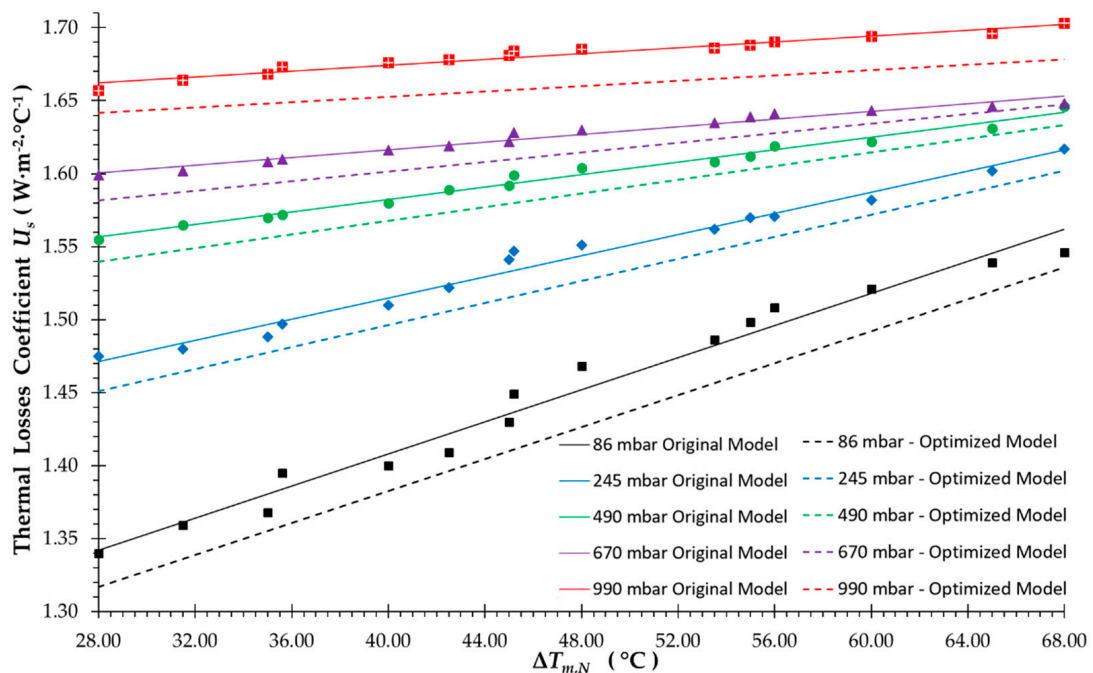


Figure 10. Variation of the thermal loss coefficient for the optimized and reference ICS models.

In both Figures 9 and 10, the solid lines represent the variation of the mean daily efficiency and thermal losses coefficient for the original models, while the dash lines represent the corresponding variations for the optimized models. It is important to note that the variations in both mean daily efficiencies and thermal losses coefficients for the original models, depicted with the solid lines, were obtained based on experimental test results. The experimental results in both mean daily efficiencies and thermal losses coefficients are additionally pointed out with several markers in the above figures. Figure 9 shows that the systems with initial pressure “670 mbar” and “990 mbar” perform better than the rest of them. The systems with the lowest values in the mean daily efficiency and the thermal loss coefficient are the “245 mbar” and “86 mbar”, respectively. Compared with the original models, as depicted in Figures 9 and 10, the designed systems appear to have higher mean daily efficiency and a slightly lower thermal loss coefficient. For all the above, it can be considered that ICS systems of initial pressure “670 mbar” and “990 mbar” approach the optimal thermal behaviour, thus taking into account the daily and the night operation of them. These findings are consistent with the results obtained by the experimental study of the original ICS devices [26,27].

Table 2 presents the fabrication costs of the five cases studied through the algorithm. The specific table summarizes the fabrication cost that was derived by the code for each separate case, the fabrication cost of the reference ICS model [35], and the differences between the optimized cases and the original ones.

Table 2. Fabrication costs derived by the GUI environment and cost of the reference ICS.

Cases for Initial Pressure (in mbar)	Fabrication Costs (Euros)		Cost Differences (€)
	Optimized ICS Unit	Reference ICS Unit	
990 ± 23	210.74	255.12	44.38
670 ± 16	208.98	255.12	46.14
490 ± 11	207.00	255.12	48.12
245 ± 6	202.45	255.12	52.67
86 ± 2	195.12	255.12	60.00

It can be seen from Table 2 that the “990 mbar” case exhibits the minimum difference (between the cost of the optimized ICS unit and the cost of the original system), while the “86 mbar” depicts the maximum difference. The “670 mbar” case presents the second minimum difference after the “990 mbar” option. Since the method simulates the domestic hot water needs of a house with four occupants, the most suitable cases correspond to five ICS systems “670 mbar” and “990 mbar” with fabrication costs of EUR 210.74 and 208.98 per unit, respectively. When taking into account the analysis of the previous paragraphs and the information provided from Table 2, the “990” and “670 mbar” cases represent more accurately the optimum solution of the problem, because they are a compromise between the maximum efficiency and the variation in the fabrication cost for the designed ICS unit. The above cases mostly approximate the optimum solution of Equation (4) thus, they will be selected.

Next, the energy and cost analysis (for systems installed in a house with four occupants), including the possible number of the designed units for those selected by the algorithm’s best cases (670 mbar and 990) will be implemented. The redesigned cases 670 mbar and 990 mbar are renamed to ICS 670 and ICS 990, respectively, while all cases for the original models are renamed to ICS original. A summary of the results for the redesigned systems, depicting information about the optimum dimensions of the parabolic concentrator, the number of ICS units which will be installed in the building, the produced annual thermal energy, the annual emission reduction, and the production cost of the designed systems, are presented in Table 3. The water storage volume, for the proposed ICS models was considered to be 48.18ℓ, following the design construction details [26,27,49]. In addition, in order to validate the dependency of results with the variations in climate

conditions, three different locations in southern, central, and northern Greece were considered (Chania, Athens, and Thessaloniki, respectively). For simplicity, the columns of Table 3 are classified using the keywords C: Chania, A: Athens, T: Thessaloniki. In Table 4, the environmental impacts in the production and installation phase are presented. Both redesigned best cases systems behave the same for all components.

Table 3. Number of ICS units produced thermal energy, greenhouse gas emissions and optimum dimensions of the reflector for the two selected, by the algorithm, best cases for three different geographic locations in Greece.

Systems	Number of ICS Units			Produced Thermal Energy (MWh/Year)			Emission Reduction (tn CO ₂ /Year)			Production Cost (EUR)			Total CPC Width (m)		
	C	A	T	C	A	T	C	A	T	C	A	T	C	A	T
ICS 670	3	4	4	4.08	4.88	4.80	0.81	0.96	0.92	583.35	835.92	854.28	1.168	1.262	1.390
ICS 990	3	4	4	4.20	5.04	4.96	0.90	1.04	1.00	593.22	842.96	861.20	1.193	1.295	1.423

Table 4. Environmental impacts in fabrication and installation phases for the two selected, by the algorithm, best cases, following the description of the + and—rating sequence in Section 2.4.

Systems	Reflector Pollutants	Tank Pollutants	Insulation Pollutants	Outer Cover Pollutants
ICS 670	— + +	+ + +	— + +	— + +
ICS 990	— + +	+ + +	— + +	— + +

According to Table 3, the designed models try to reach the producing energy of the “Athens” area [27], thus modifying the reflector’s geometry. Based on that assumption, the program decreases the size of the reflector, the production cost, and the number of installed units in the building that will be installed in southern locations. On the other hand, the algorithm predicts more units for northern locations with a larger reflector width and therefore higher production costs. The next step is the evaluation of the profitability for one unit of these studied cases, considering only the geographic location of Chania (Crete), which appears to be the most cost-effective and energy-efficient proposed solution by the algorithm, which will be attempted using the economic analysis procedure of the GUI environment. Table 5 presents the economical results for the redesigned systems.

Table 5. Aggregate economical results of the redesigned systems for the two best cases/units (considering the geographic location of Chania, Crete).

Systems	Simple Payback Period (Years)	NPV (€)
ICS original	5.9	118.00
ICS 670	4.4	146.24
ICS 990	4.3	154.17

The aggregate results for the produced thermal energy and the net annual emission reduction for the original and best-redesigned two models are presented in Figure 11. The results refer to one unit for each model.

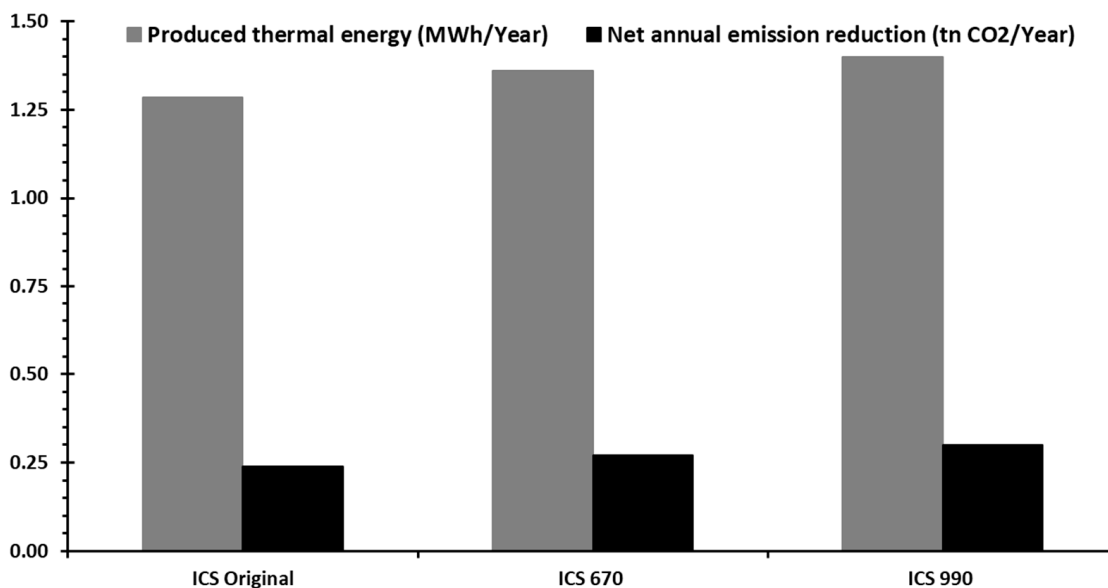


Figure 11. Aggregate results for the produced thermal energy and the net annual emissions reduction during operation mode of all the studied systems.

It is evident from Figure 11 that system ICS 990 demonstrates very high energy and environmental performance compared to the rest of the ICS systems and constitutes the best choice for the design of specific devices, if taking into account only the maximization of the producing thermal energy. Although the original ICS system presents comparable ranges to the optimum ICS systems (ICS 670 and ICS 990) for both produced thermal energy and net annual emission reduction, the latter operate marginally better. The optimum configuration of these units contributes to relatively low environmental impacts during operation mode, depending on the existing thermal energy production. The system ICS 670 follows and corresponds to the optimum configuration for the designed ICS vessels because it combines energy and environmental efficiency with the minimization of the fabrication cost and the prediction of the minimum number of units. According to Table 3, the algorithm decreases the number of units for systems that will be installed in geographic locations with higher solar radiation, while it increases the corresponding units for systems installed in northern regions. In addition, it should be stressed that the redesigned systems are valuable investments against the original ICS unit, taking into account the NPV and simple payback period values, as presented in Table 5.

4. Conclusions

A detailed energy, environmental, economic, and design analysis has been presented in two stages for ICS solar thermal systems, focusing on domestic hot water applications in Greece. The prototype ICS unit is a specially designed device with an asymmetric CPC reflector that comprises two concentric cylindrical vessels in the water storage tank. The annulus between the cylinders is partially depressurized containing a small amount of water that serves as PCM material, creating a thermal transfer mechanism from the environment to the inner vessels.

In order to improve the energy, economic and environmental efficiency of the prototype ICS system, a multi-criteria optimization method has been employed. In the first stage, the design of the parabolic parts of the CPC reflector's surface (for varying climate conditions) and the evaluation of the minimum number of the units (in house with four occupants) are implemented. This process maximizes the energy and environmental performance, whilst at the same time minimising the production cost of the studied systems. Based on this optimization, new ICS systems are designed comprising a totally new geometry of the reflector's surface with optimized horizontal and vertical dimensions, as these

are evaluated by the optimum angles ψ_m and φ_m of the parabolic curves. The adopted procedure includes the design of the entire ICS system's components. In the second stage, a methodology for the formulation of the specific reflector's geometry, using the above optimization technique and CAD environment, is proposed. The results indicate that the ICS devices are cost-effective, compared to the prototype ICS units. Several tests depicted the variation of the mean daily efficiency and the thermal loss coefficient of the improved ICS devices, which differ in the initial total pressure inside the annulus. In particular, the "670 mbar" choice produces the minimum number of the designed vessels, which can operate with higher performance compared to the original system and represents the optimum solution of the design analysis.

The conducted energy, environmental and cost analysis for varying climate conditions, combined with the design analysis methodology in the second stage, indicate that the cases "670 and 990 mbar" improve the energy performance of the prototype device. The analysis suggests the installation of a lower number of units for southern regions. Based on the energy and environmental analysis, it is evident that the above cases are much more efficient and environmentally friendly during operation mode. In addition, the economic study proves that the proposed ICS devices exhibit better economical behaviour compared to the original one. The present study might serve as a guidance for the design and selection of improved ICS devices, which will be installed in buildings for domestic applications.

Author Contributions: N.A.: conceptualization, methodology, and writing the original paper; A.P.V.: results and diagrams; M.M.: methodology, writing, and editing; Y.G.C.: editing; G.P.: methodology and editing; A.T.: editing; K.V.: methodology; G.M.: editing; C.S.G.: methodology and editing; Z.F.: editing; S.P.: methodology, writing, and editing; M.S.: methodology, writing, editing, and supervision. All authors have read and agreed to the published version of the manuscript.

Funding: This research has been co-financed by the European Union and Greek national funds through the Operational Program Competitiveness, Entrepreneurship and Innovation, under the call RESEARCH—CREATE—INNOVATE (project code: T1EDK-01740).

Institutional Review Board Statement: Not applicable.

Informed Consent Statement: Not applicable.

Conflicts of Interest: The authors declare no conflict of interest.

References

1. Souliotis, M.; Tripanagnostopoulos, Y. Study of the distribution of the absorbed solar radiation on the performance of a CPC-type ICS water heater. *Renew. Energy* **2008**, *33*, 846–858. [[CrossRef](#)]
2. Tripanagnostopoulos, Y.; Souliotis, M.; Nousia, T. CPC type integrated collector storage systems. *Sol. Energy* **2002**, *72*, 327–350. [[CrossRef](#)]
3. O'Gallagher, J.J.; Snail, K.; Winston, R.; Peek, C.; Garrison, J.D. A new evacuated CPC collector tube. *Sol. Energy* **1982**, *29*, 575–577. [[CrossRef](#)]
4. Souliotis, M.; Singh, R.; Papaefthimiou, S.; Lazarus, I.J.; Andriosopoulos, K. Integrated collector storage solar water heaters: Survey and recent developments. *Energy Syst.* **2016**, *7*, 49–72. [[CrossRef](#)]
5. Singh, R.; Lazarus, I.J.; Souliotis, M. Recent developments in integrated collector storage (ICS) solar water heaters: A review. *Renew. Sust. Energy Rev.* **2016**, *54*, 270–298. [[CrossRef](#)]
6. Papaefthimiou, S.; Zopounidis, C.; Andriosopoulos, K. Editorial for the Special Issue: Recent developments in energy modeling and management. *Energy Syst.* **2016**, *7*, 1–4. [[CrossRef](#)]
7. Crawford, R.H.; Treloar, G.J.; Ilozor, B.D.; Love, P.E.D. Comparative greenhouse emissions analysis of domestic solar hot water systems. *Build. Res. Inf.* **2003**, *31*, 34–47. [[CrossRef](#)]
8. Kalogirou, S.A. Thermal performance, economic and environmental life cycle analysis of thermosiphon solar water heaters. *Sol. Energy* **2009**, *83*, 39–48. [[CrossRef](#)]
9. Hang, Y.; Qu, M.; Zhao, F. Economic and environmental life cycle analysis of solar hot water systems in the United States. *Energy Build.* **2012**, *45*, 181–188. [[CrossRef](#)]
10. Colle, S.; De Abreu, S.L.; R  ther, R. Uncertainty in economical analysis of solar water heating and photovoltaic systems. *Sol. Energy* **2001**, *70*, 131–142. [[CrossRef](#)]
11. Ardente, F.; Beccali, G.; Cellura, M.; Lo Brano, V. Life cycle assessment of a solar thermal collector. *Renew. Energy* **2005**, *30*, 1031–1054. [[CrossRef](#)]

12. Crawford, R.H.; Treloar, G.J. Net energy analysis of solar and conventional domestic hot water systems in Melbourne, Australia. *Sol. Energy* **2004**, *76*, 159–163. [[CrossRef](#)]
13. Jankura, A.; Sekret, R. Life cycle assessment of the use of phase change material in an evacuated solar tube collector. *Energies* **2021**, *14*, 4146.
14. Karasu, H.; Dincer, I. Life cycle assessment of integrated thermal energy storage systems in buildings: A case study in Canada. *Energy Build.* **2021**, *217*, 109940. [[CrossRef](#)]
15. Lamnatou, C.; Chemisana, D. Concentrating solar systems: Life Cycle Assessment (LCA) and environmental issues. *Renew. Sust. Energy Rev.* **2017**, *78*, 916–932. [[CrossRef](#)]
16. Lamnatou, C.; Cristofari, C.; Chemisana, D.; Canaletti, J.L. Building-integrated solar thermal systems based on vacuum-tube technology: Critical factors focusing on life-cycle environmental profile. *Renew. Sust. Energy Rev.* **2016**, *65*, 1199–1215. [[CrossRef](#)]
17. Lamnatou, C.; Motte, F.; Notton, G.; Chemisana, D.; Cristofari, C. Cumulative energy demand and global warming potential of a building-integrated solar thermal system with/without phase change material. *J. Environ. Manag.* **2018**, *212*, 301–310. [[CrossRef](#)]
18. Hobson, P.A.; Norton, B. A design nomogram for direct thermosyphon solar-energy water heaters. *Sol. Energy* **1989**, *43*, 85–95. [[CrossRef](#)]
19. Gordon, J.M.; Rabl, A. Design, analysis and optimization of solar industrial process heat plants without storage. *Sol. Energy* **1982**, *28*, 519–530. [[CrossRef](#)]
20. Frei, U.; Vogelsanger, P. Solar Thermal Systems for Domestic Hot Water and Space Heating. Report of SPF Institut für Solartechnik Prüfung Forschung. 2000, pp. 1–12. Available online: https://www.researchgate.net/publication/238741144_SOLAR_THERMAL_SYSTEMS_FOR_DOMESTIC_HOT_WATER_AND_SPACE_HEATING (accessed on 8 January 2022).
21. Lund, P.D.; Peltola, S.S. SOLCHIPS-A fast predesign and optimization tool for solar heating with seasonal storage. *Sol. Energy* **1992**, *48*, 291–300. [[CrossRef](#)]
22. Abdel-Malek, L. Optimum design of solar water heating systems. *Comput. Oper. Res.* **1985**, *12*, 219–225. [[CrossRef](#)]
23. De Winter, F. Optimum Designs for Solar Water Heating Equipment for the Single Family Home. In Proceedings of the +IV Conferencia Latino Americana de Energía Solar (IV ISES CLA) y XVII Simposio Peruano de Energía, Cusco, Peru, 1–5 November 2010.
24. Ko, M.J. Analysis and Optimization Design of a Solar Water Heating System Based on Life Cycle Cost Using a Genetic Algorithm. *Energies* **2015**, *8*, 11380–11403. [[CrossRef](#)]
25. Patrčević, F.; Dović, D.; Horvat, I.; Filipović, P. A Novel Dynamic Approach to Cost-Optimal Energy Performance Calculations of a Solar Hot Water System in an nZEB Multi-Apartment Building. *Energies* **2022**, *15*, 509. [[CrossRef](#)]
26. Souliotis, M.; Quinlan, P.; Smyth, M.; Tripanagnostopoulos, Y.; Zacharopoulos, A.; Ramirez, M.; Yianoulis, P. Heat retaining integrated collector storage solar water heater with asymmetric CPC reflector. *Sol. Energy* **2011**, *85*, 2474–2487. [[CrossRef](#)]
27. Souliotis, M.; Papaefthimiou, S.; Caouris, Y.G.; Zacharopoulos, A.; Quinlan, P.; Smyth, M. Integrated collector storage solar water heater under partial vacuum. *Energy* **2017**, *139*, 991–1002. [[CrossRef](#)]
28. Haillot, D.; Py, X.; Goetz, V.; Benabdelkarim, M. Storage composites for the optimisation of solar water heating systems. *Chem. Eng. Res. Des.* **2008**, *86*, 612–617. [[CrossRef](#)]
29. Eames, P.C.; Griffiths, P.W. Thermal behaviour of integrated solar collector/storage unit with 65 °C phase change material. *Energy Convers. Manag.* **2006**, *47*, 3611–3618. [[CrossRef](#)]
30. Al-Hinti, I.; Al-Ghandoor, A.; Maaly, A.; Abu Naqera, I.; Al-Khateeb, Z.; Al-Sheikh, O. Experimental investigation on the use of water-phase change material storage in conventional solar water heating systems. *Energy Convers. Manag.* **2010**, *51*, 1735–1740. [[CrossRef](#)]
31. Chaabane, M.; Mhiri, H.; Bournot, P. Thermal performance of an integrated collector storage solar water heater (ICSSWH) with phase change materials (PCM). *Energy Convers. Manag.* **2014**, *78*, 897–903. [[CrossRef](#)]
32. De Beijer, H.A. Product development in solar water heating. *Renew. Energy* **1998**, *15*, 201–204. [[CrossRef](#)]
33. Pugsley, A.; Smyth, M.; Mondol, J.D.; Zacharopoulos, A.; Di Mattia, L. Experimental Characterisation of a Flat Panel Integrated-Collector-Storage Solar Water Heater Featuring a Photovoltaic Absorber and a Planar Liquid-Vapour Thermal Diode. In Proceedings of the 11th EuroSun 2016, Palma, Spain, 11–14 October 2016; pp. 1–12.
34. Rhee, J.; Campbell, A.; Mariadass, A.; Morhous, B. Temperature stratification from thermal diodes in solar hot water storage tank. *Sol. Energy* **2010**, *84*, 507–511. [[CrossRef](#)]
35. Arnaoutakis, N.; Souliotis, M.; Papaefthimiou, S. Comparative experimental Life Cycle Assessment of two commercial solar thermal devices for domestic applications. *Renew. Energy* **2017**, *111*, 187–200. [[CrossRef](#)]
36. ISO 14040:2006; Environmental Management—Life Cycle Assessment—Principles and Framework. ISO: Geneva, Switzerland, 2006. Available online: <https://www.iso.org/standard/37456.html>(accessed on 8 January 2022).
37. ISO 14044:2006; Environmental Management—Life Cycle Assessment—Requirements and Guidelines. ISO: Geneva, Switzerland, 2006. Available online: <https://www.iso.org/standard/38498.html>(accessed on 8 January 2022).
38. SimaPro. The World’s Leading LCA Software. Available online: <https://simapro.com/> (accessed on 8 January 2022).
39. Ecoinvent. Available online: <https://www.ecoinvent.org/> (accessed on 8 January 2022).
40. Agency for Toxic Substances and Disease Registry. Available online: <https://www.atsdr.cdc.gov/> (accessed on 8 January 2022).
41. Souliotis, M.; Tripanagnostopoulos, Y. Experimental study of CPC type ICS solar systems. *Sol. Energy* **2004**, *76*, 389–408. [[CrossRef](#)]
42. Engineering ToolBox. Available online: <https://www.engineeringtoolbox.com/> (accessed on 8 January 2022).
43. Rabl, A. Solar concentrators with maximal concentration for cylindrical absorbers. *Appl. Opt.* **1976**, *15*, 1871. [[CrossRef](#)]

44. Arnaoutakis, N.; Milousi, M.; Papaefthimiou, S.; Fokaides, P.A.; Caouris, Y.G.; Souliotis, M. Life cycle assessment as a methodological tool for the optimum design of integrated collector storage solar water heaters. *Energy* **2019**, *182*, 1084–1099. [CrossRef]
45. RETScreen. Natural Resources Canada. Available online: <https://www.nrcan.gc.ca/maps-tools-publications/tools/data-analysis-software-modelling/retscreen/7465> (accessed on 8 January 2022).
46. Lin, G.C.I.; Nagalingam, S.V. *CIM Justification and Optimisation*; Taylor & Francis; CRC Press: London, UK, 2000.
47. Khan, M.Y. *Theory and Problems in Financial Management*. Available online: <https://www.bookdepository.com/Theory-Problems-Financial-Management-M-Y-Khan/9780074636831> (accessed on 8 January 2022).
48. William, W.A.; Deren, B.J.; D'Silva, E.H. *The Economics of Project Analysis: A Practitioner's Guide*; Economic Development Institute of the World Bank, World Bank Publications: Washington, DC, USA, 1991.
49. Tripanagnostopoulos, Y.; Souliotis, M. Integrated collector storage solar Systems with asymmetric CPC reflectors. *Renew. Energy* **2004**, *29*, 223–248. [CrossRef]
50. Schaum's Mathematical Handbook of Formulas And tables. Available online: <https://epdf.pub/schaums-mathematical-handbook-of-formulas-and-tablesdc2f8603272491941b362853bbce940385159.html> (accessed on 8 January 2022).
51. McCleary, J. *Geometry from a Differentiable Viewpoint*; Cambridge University Press: Cambridge, UK, 2012.
52. Kuester, J.L.; Mize, J.H. *Optimization Techniques with Fortran*; Mc Graw-Hill: New York, NY, USA, 1973.
53. Spendley, W.; Hext, G.R.; Himsworth, F.R. Sequential Application of Simplex Designs in Optimisation and Evolutionary Operation. *Technometrics* **1962**, *4*, 441. [CrossRef]
54. AAMA-Glass Standards and Guidelines. Available online: <https://aamanet.org/pages/glass-standards-and-guidelines> (accessed on 8 January 2022).
55. Materials Science and Engineering. MIT Open Course Ware. Free Online Course Materials. Available online: <https://ocw.mit.edu/courses/materials-science-and-engineering/> (accessed on 8 January 2022).
56. Plastics-The Home of Plastics. Available online: <https://plasticer.de/> (accessed on 8 January 2022).
57. Velmurugan, V.; Srihar, K. Prospects and scopes of solar pond: A detailed review. *Renew. Sust. Energy Rev.* **2008**, *12*, 2253–2263. [CrossRef]
58. Review of Solar Radiation Estimation and Solar Data Banks Elaboration Methodologies over Greece. Available online: https://www.researchgate.net/publication/230710390_Review_of_Solar_Radiation_estimation_and_Solar_Data_Banks_elaboration_methodologies_over_Greece (accessed on 8 January 2022).